

Yu.N. Dnestrovskij, V.F. Andreev, A.V. Danilov, A.Yu. Dnestrovskij,  
S.V. Cherkasov, S.E. Lysenko, T.C. Hender, C.M. Roach, I.A. Voitsekhovich,  
and JET EFDA contributors

# Canonical Profiles and Transport Model for the Toroidal Rotation in Tokamaks

“This document is intended for publication in the open literature. It is made available on the understanding that it may not be further circulated and extracts or references may not be published prior to publication of the original when applicable, or without the consent of the Publications Officer, EFDA, Culham Science Centre, Abingdon, Oxon, OX14 3DB, UK.”

“Enquiries about Copyright and reproduction should be addressed to the Publications Officer, EFDA, Culham Science Centre, Abingdon, Oxon, OX14 3DB, UK.”

The contents of this preprint and all other JET EFDA Preprints and Conference Papers are available to view online free at [www.iop.org/Jet](http://www.iop.org/Jet). This site has full search facilities and e-mail alert options. The diagrams contained within the PDFs on this site are hyperlinked from the year 1996 onwards.

# Canonical Profiles and Transport Model for the Toroidal Rotation in Tokamaks

Yu.N. Dnestrovskij<sup>1</sup>, V.F. Andreev<sup>1</sup>, A.V. Danilov<sup>1</sup>, A.Yu. Dnestrovskij<sup>1</sup>, S.V. Cherkasov<sup>1</sup>,  
S.E. Lysenko<sup>1</sup>, T.C. Hender<sup>2</sup>, C.M. Roach<sup>2</sup>, I.A. Voitsekhovich<sup>2</sup>,  
and JET EFDA contributors\*

*JET-EFDA, Culham Science Centre, OX14 3DB, Abingdon, UK*

<sup>1</sup>*RRC 'Kurchatov Institute', Tokamak Physics Institute, Moscow 123182, Russia*

<sup>2</sup>*EURATOM/CCFE Fusion Association, Culham Science Centre, Abingdon, Oxon, OX14 3DB, UK*

*\* See annex of F. Romanelli et al, "Overview of JET Results",  
(23rd IAEA Fusion Energy Conference, Daejeon, Republic of Korea (2010)).*



## ABSTRACT.

The equilibrium equation for a rotating plasma is constructed supposing the thermal Mach number is much less than unity. The canonical profile of angular rotation velocity is defined as the profile which minimizes the total plasma energy while conserving toroidal current and obeying the equilibrium condition. The transport model based on this canonical profile, with stiffness calibrated by JET data, reasonably describes the velocity of the forced toroidal rotation. The RMS deviations of the calculated rotation profiles from the experimental ones do not exceed 10-15%. The developed model is also applied to the modeling of MAST rotation.

## 1. INTRODUCTION

Toroidal rotation of plasma occurs in all tokamaks. In accordance with torque mechanism it can be divided for modern tokamaks into two types:

1) intrinsic rotation, for which the rotation velocity  $v_t$  is usually limited in experiment by the condition:

$$v_t < 20 - 40 \text{ km/s} \quad (1)$$

2) forced rotation with rather large velocities

$$v_t < 200 - 400 \text{ km/s} \quad (2)$$

The level of forced rotation is determined by the input of external angular momentum (torque)  $T$ . The most widespread source of torque now is neutral beam injection [1-2]. Below we discuss forced rotation only.

In this work we solve two main problems. At first we construct the canonical profile for the toroidal angular frequency  $\omega$  using the variation principle proposed in [3]. Then we develop the linear transport model for the toroidal momentum  $L = nm_i R v_t$  based on this canonical profile. Here  $n$  is the plasma density,  $R$  is the distance from the major axis of torus,  $m_i$  is the ion mass. The stiffness of the frequency profile is found by the simulation of the set of 11 JET H-mode shots. The full model includes the nonlinear equations for the electron and ion temperatures,  $T_e$ ,  $T_i$ , and plasma density,  $n$ , and the linear equation for  $\omega$ . The nonlinear transport model includes the External Transport Barrier (ETB) [4]. The linear model for  $\omega$  does not include the ETB and uses the experimental boundary conditions. The RMS deviations of the calculated angular frequency profiles from the experimental ones do not exceed 10-15%.

The paper is organized as follows. In the Section 2 the equilibrium equation for rotating plasma is obtained. The variation problem concerning plasma energy minimum is considered in the Section 3. The canonical profile of the angular frequency is constructed in Section 4. In the Section 5 the transport model is developed. The Section 5.1 is devoted to the linear model concerning the momentum. In the Section 5.2 we remind the nonlinear model for the temperatures and density. The stiffness of the angular frequency profile is discussed in Section 5.3. The results of calculations for JET and MAST are considered in the Section 6. The conclusion reviews shortly the main results of the paper.

## 2. THE EQUILIBRIUM EQUATION FOR ROTATING PLASMA

The velocity of toroidal rotation is as follows:  $v_t = v_t(\psi, R) = \omega R$ , where  $\omega = \omega(\psi)$  is an angular frequency,  $\psi$  is the poloidal magnetic flux. The equilibrium equation for rotating plasma can be written as

$$\Delta^* \psi = -R j_\phi = -(FF' + R^2 p') \quad p = p(\psi, R) \quad (3)$$

where  $p$  is a plasma pressure,  $F$  is the toroidal field function  $F = RB_t$ . In sections 2 and 3 the prime designates the derivative with respect to  $\psi$ . The dependence on  $R$  has to satisfy the condition

$$\partial p / \partial R = \rho_m v_t^2 / R = \rho_m R \omega^2. \quad (4)$$

Here  $\rho_m$  is the mass density of plasma ( $\rho_m = n m_i$ ). We suppose that the kinetic energy of plasma rotation is much less than the thermal energy

$$\rho_m v_t^2 / 2 \ll p, \quad \text{or} \quad v_t^2 \ll v_T^2 \quad (M^2 = v_t^2 / v_T^2 \ll 1). \quad (5)$$

Here  $v_T$  is the ion thermal velocity,  $M$  is the thermal Mach number. We choose the simplest form of the function  $p(\psi, R)$ , which satisfies the condition (4) as:

$$p = p_0(\psi) + R^2 / R_0^2 p_1 \quad (6)$$

where  $p_0(\psi)$  is the usual thermal pressure for non rotating plasma

$$p_1 = (R_0^2 / 2) \rho_m \omega^2 \quad (7)$$

and  $R_0$  is a major radius of plasma. From relation (5)

$$p_1 \ll p_0, \quad (8)$$

so in the expression for  $p_1$  (7) we can accept that  $\rho_m$  and  $p_1$  are independent on  $R$ . Therefore  $n = n(\psi)$  and  $p_1 = p_1(\psi)$ . As a result, the equilibrium equation (3) has the form

$$\Delta^*\psi = -R j_\phi = -\{FF' + R^2(p_0' + R^2/R_0^2 p_1')\} \quad (9)$$

### 3. CANONICAL EQUILIBRIUM EQUATION

Now we consider the variation problem. The canonical profiles of pressure, rotation and poloidal current can be defined as those minimizing the total plasma energy while conserving the toroidal current and satisfying equation (9). The total plasma energy  $W$  and the toroidal current  $I_p$  are

$$W = \int_V dV \{ [F^2 + (\nabla\psi)^2]/(2R^2) + 3/2 p + \rho_m v_t^2/2 \}, \quad (10)$$

$$I_p = 1/(2\pi R) \int_V dV (FF' + R^2 p')/R \quad (11)$$

The generalized Lagrange functional has the form:

$$\Phi = W - 2\pi\lambda I_p$$

Its first variation in the extreme point should be equal to zero

$$\begin{aligned} \delta\Phi = \int_V dV \delta\psi \{ [(FF' - \Delta^*\psi)/R^2 + 3/2 (p_0 + R^2/R_0^2 p_1)'] - \\ - \lambda[(F'F' + FF'')/R^2 + (p_0 + R^2/R_0^2 p_1)'] \} = 0 \end{aligned} \quad (12)$$

From this and (9) we obtain the 2D Euler equation

$$[2FF'/R^2 - \lambda[(FF')'/R^2] + (5/2 p_0' - \lambda p_0'') + R^2/R_0^2 [5/2 p_1' - \lambda p_1'']] = 0 \quad (13)$$

The second term in (13) is constant over the magnetic surface, but other terms are not. From this we obtain three independent 1D equations

$$2FF' - \lambda(FF')' = 0, \quad 5/2 p_0' - \lambda p_0'' = 0, \quad 5/2 p_1' - \lambda p_1'' = 0 \quad (14)$$

Here first and second equations coincide with corresponding equations for a stationary plasma [3]. The third equation for  $p_1$  coincides with the equation for  $p_0$ . Thus, the canonical profile for the function  $p_1 = (R_0^2/2) \rho_m \omega^2$  coincides with the canonical profile for the function  $p_0$ .

The solutions of equations (14) are the functions

$$FF' = C_F \exp(\psi/\lambda), \quad p_0' = C_p \exp(5\psi/4\lambda), \quad p_1' = C_{p1} \exp(5\psi/4\lambda) \quad (15)$$

Substituting (15) to (9), we obtain the equation for the canonical equilibrium:

$$\Delta^* \psi = -R j_\phi = - \{ C_F \exp(\psi/\lambda) + C_p R^2 \exp(5\psi/4\lambda) (p_0(0) + R^2 \rho_{m0} \omega_0^2/2) \} \quad (16)$$

Here we define that on the magnetic axis  $\psi = 0$ ,  $\rho_{m0} = \rho_m(0)$ ,  $\omega_0 = \omega(0)$ . The parameters  $C_F$ ,  $C_p$  and  $\lambda$  have to be defined from additional conditions, for example:

$$\psi|_S = \psi_a, \quad q(0) = q_0 \quad I_p \text{ is prescribed} \quad (17)$$

In the case of a circular cylinder Eq. (16) has the form:

$$-\Delta \psi = C_F \exp(\psi/\lambda) + C_p \exp(5\psi/4\lambda) \quad (18)$$

If we put  $C_p = 0$  (low plasma pressure), we obtain

$$1/r \, d/dr (r \, d\psi/dr) = \psi'' + \psi'/r = -C_F \exp(\psi/\lambda) \quad (19)$$

The solution of this equation has the form:

$$\psi/\lambda = -\ln(1+Dr^2)^2 \quad (20)$$

Substituting (20) into (19), we find the link between parameters  $D$ ,  $\lambda$  and  $C_F$ . Then it is straightforward to find the poloidal magnetic field  $B_\theta$ ,  $\mu = 1/q$  and the current density  $j$ :

$$B_\theta = C_F/2 [r/(1+Dr^2)], \quad \mu = R B_\theta/(rB_0) = \mu_0/(1+Dr^2), \quad j = j_0/(1+Dr^2)^2 \quad (21)$$

The constant  $D$  is defined by boundary conditions. Expressions (21) coincide with Kadomtsev's formulae based on the minimization of the poloidal magnetic energy functional [5]. This coincidence is a basis for conclusions given in the following section.

#### 4. CANONICAL PROFILE FOR ANGULAR ROTATION FREQUENCY

Taking into account that the canonical profiles are defined with accuracy of multiplier and using the result from previous section that  $p_{c1} \propto p_{c0}$ , we obtain

$$p_{c1} \propto p_{c0} \propto \rho_{mc} \omega_c^2 \propto n_c \omega_c^2 \propto n_c T_c \quad (22)$$

therefore

$$T_c \propto \omega_c^2 \quad (23)$$

The canonical profiles here are denoted by the subscript "c". The canonical profile for temperature was defined in our previous papers [6, 7]. In particular there was shown that  $T_c \propto p_c^{2/3}$ . From this we obtain



$$\omega_c \propto T_c^{1/2} \propto p_{0c}^{1/3} \quad (24)$$

In the transport model we will use the logarithmic derivatives of different variables. From (24), they are linked by following relations

$$\omega_c'/\omega_c = 1/3 p_{0c}'/p_{0c} = 1/2 T_c'/T_c \quad (25)$$

Here and below the prime now denotes the derivative over the dimensional radial coordinate  $\rho$ , which defines the magnetic surface ( $0 < \rho < \rho_{\max}$ ). The canonical profiles for the current and pressure were defined in [6, 7].

## 5. TRANSPORT MODEL OF CANONICAL PROFILES

### 5.1. LINEAR MODEL FOR TOROIDAL ROTATION

The specific angular momentum is defined as:

$$L = n m_i R v_t = n m_i R^2 \omega \quad (26)$$

We assume that the radial flux of the angular momentum  $q_\omega$  is proportional to the difference between the relative gradient of calculated momentum and the relative gradient of canonical momentum (similarly to the heat and particle fluxes in [7 - 9]). In the linear model this flux is equal to

$$q_\omega = - n m_i R^2 \chi_\omega^{\text{PC}} \omega (\omega'/\omega - \omega_c'/\omega_c) \quad (27)$$

The equation for momentum has the form

$$\partial/\partial t L = - \text{div}_\rho (q_\omega) + t_m, \quad t_m = n \Phi R \quad (28)$$

where  $t_m$  is a specific torque,  $\Phi$  is the force applied to a mass corresponding to  $1 \text{ m}^3$ . After integration of (28) over the plasma volume we obtain

$$\partial L_0/\partial t = - L_0/\tau_\omega + T, \quad (29)$$

where

$$L_0 = \int_V dV L, \quad T = \int_V dV t_m \quad (30)$$

are the total angular momentum and total torque,  $L_0/\tau_\omega = - q_{\omega a}$ ,  $\tau_\omega$  is the angular momentum confinement time:  $\tau_\omega = L_0 / (T - \partial L_0/\partial t)$ . In the steady state

$$\tau_\omega = L_0 / T \quad (31)$$

Usually in the experiment  $\tau_\omega$  is close to the energy confinement time  $\tau_E$ .

## 5.2. NONLINEAR MODEL FOR THE ELECTRON AND ION TEMPERATURES AND PLASMA DENSITY

This model was described and validated in [4, 10]. The heat and particle fluxes,  $q_\alpha$  ( $\alpha = e, i$ ),  $\Gamma$ , are as follows:

$$q_\alpha = -n\chi_\alpha^{\text{PC}} T_\alpha (T_\alpha'/T_\alpha - T_c'/T_c) H(-[T_\alpha'/T_\alpha - T_c'/T_c]) F_\alpha - n\chi_\alpha^0 T_\alpha' + 3/2 \Gamma T_\alpha \quad (32)$$

$$\Gamma = -D n (p_e'/p_e - p_c'/p_c) F_e F_i - D^0 n' + \Gamma^{\text{neo}}, \quad (33)$$

where  $T_\alpha$  and  $n$  are the temperatures and density to be determined,  $T_c$  and  $p_c$  are the canonical profiles of temperature and pressure,  $\chi_\alpha^{\text{PC}}$  and  $D$  are stiffness coefficients,  $\Gamma^{\text{neo}} = n v^{\text{neo}}$ ,  $H(x)$  is the Heaviside function,  $\rho$  is a radial coordinate ( $0 < \rho < \rho_{\text{max}}$ ). The values of  $\chi_\alpha^{\text{PC}}$  were found earlier by the comparison of calculations with experiment [9, 6]:

$$\chi_\alpha^{\text{PC}} = C_{T\alpha} (1/M) (a/R)^{0.75} q(\rho = \rho_{\text{max}}/2) q_{\text{cyl}} (T_c(\rho = \rho_{\text{max}}/4))^{1/2} (3/R)^{1/4} (1/B_0) \bar{n}/n \quad (34)$$

where  $a$  and  $R$  are minor and major radii,  $B_0$  is the toroidal magnetic field,  $M$  is ion mass number,  $q_{\text{cyl}} = B_0 a^2 / 2 I_p R$ ,  $I_p$  is the plasma current. We use everywhere  $n$ ,  $I_p$ ,  $P_{\text{tot}}$ ,  $R$ ,  $T_{e,i}$  and  $\chi$  in  $10^{19} \text{m}^{-3}$ , MA, MW, m, keV,  $\text{m}^2/\text{s}$  respectively,  $\langle \dots \rangle$  denotes volume-averaging,  $P_{\text{tot}}$  is the auxiliary power deposited into plasma. We also set [4, 8]

$$\chi_i^0 (\text{m}^2/\text{s}) = 0.46 P_{\text{tot}} / (\langle n \rangle I_p), \quad \chi_e^0 = \chi_i^0 \{4.5 (T_e)^{1/2} / R\}, \quad D^0 = 0.05 \quad (35)$$

$$D = C_n \chi_e^{\text{PC}}, \quad C_n = 0.08 - 0.1, \quad D^0 = 0.05 \quad (36)$$

The values of  $\chi_\alpha^0$  and  $D^0$  are much smaller than  $\chi_\alpha^{\text{PC}}$  and  $D$ , but they play an essential role inside the transport barriers. We use also the following boundary condition for canonical profile [4]:  $\mu_c(0) = (3.5 - 4) \mu_c(a)$ , where the value of  $\mu_c(a)$  is defined by the solution of the equilibrium Grad-Shafranov equation.

To describe the barrier formation we use the possibility of bifurcation due to nonlinearities in transport equations [10]. Such nonlinearity is included in (32)-(33) using the function  $F_\alpha$  as follows:

$$F_\alpha = \exp(-z_{p\alpha}^2 / 2z_0^2), \quad (37)$$

where  $z_{p\alpha} = -(a \rho_{\text{max}} / \rho) (p_\alpha' / p_\alpha - p_c' / p_c)$  is a dimensionless “distance” between the electron or ion pressure profiles and the canonical pressure profile. The form of  $F_\alpha$  means that the

transport barrier occurs, when the distance  $z_{p\alpha}$  exceeds the critical gradient  $z_0$ :  $|z_{p\alpha}| > z_0$ . Note that inside the transport barrier  $F_\alpha \ll 1$  and the first terms in fluxes (32)-(33) will be small, but outside this region  $F_\alpha \approx 1$ . In the transient regime the parameter  $z_0$  determines the L-H transition threshold, but at the steady-state it determines the width of transport barrier. The range of  $z_0$  for different devices was explored in [10]:  $z_0 = 6-9$ . A more precise estimate of  $z_0$  is only essential for the determination of the threshold power of the L-H transition. A rough estimate of  $z_0$  is sufficient to describe the developed H-mode. Here we put  $z_0 = 8$ . With this choice the ETB width, which arises as a result of bifurcation, usually equals to 3-5% of minor plasma radius - this value does not contradict experiment. Note that the transport model described in (32)-(37) does not include the effects of rotation on the transport properties of plasma. Such effects were discovered many years ago in experiment and were described recently in [11, 12].

### **5.3. TRANSPORT COEFFICIENT FOR THE LINEAR MODEL OF ROTATING PLASMA**

We assume that the stiffness of the angular frequency profile  $\chi_\omega^{\text{PC}}$  is proportional to the stiffness of the electron temperature profile:

$$\chi_\omega^{\text{PC}} = C_\omega \chi_e^{\text{PC}}, \quad (38)$$

where  $\chi_e^{\text{PC}}$  is defined by (34). We determined  $C_\omega$  using 11 JET shots from the International Multi-tokamak Confinement Profile database [13] (Table 1). The transport equations were solved in the interval ( $0 < \rho < \rho_{\text{max}}$ ). Boundary conditions at the point  $\rho = \rho_{\text{max}}$  are taken from the experiment:  $\omega(\rho_{\text{max}}) = 8 - 22$  (krad/s). Due to errors in experimental values of  $\omega(\rho_{\text{max}})$ , we have chosen  $\omega(\rho_{\text{max}})$  to optimise the solution of the equation for  $\omega$  to fit the experimental values of  $\omega_{\text{exp}}$  in the zone  $\rho/\rho_{\text{max}} \sim 0.8 - 0.9$ . For each shot we optimize  $C_\omega$  to give the best fit to experimental measurements during the steady-state phase of discharge. The results of calculations may be approximated by formula:

$$C_\omega = 1/n^{1/3} \quad (n \text{ in } 10^{19} \text{ m}^{-3}) \quad (39)$$

We see that at high densities the rotation stiffness is rather less than the electron temperature stiffness. We will assess the accuracy of the simulation using the RMS deviations between calculated and measured profiles. The temperature deviation may be written as:

$$d_2T = \left\{ (1/N) \sum_{k=1}^N \left[ \frac{T_k^{calc} - T_k^{exp}}{T_k^{exp}} \right]^2 \right\}^{1/2} \quad (40)$$

Similar formulae are used for density and angular frequency. Although the experimental data obtained by TRANSP are finite over the whole plasma cross section, there are really few measurements of the velocity at  $\rho > 0.8 \rho_{max}$ . There is also the influence of ELMs at the plasma periphery that is not included in our model. Therefore we only sum in (40) over the region ( $0 < \rho < 0.8 \rho_{max}$ ).

## 6. RESULTS OF CALCULATIONS

The calculated and experimental profiles of angular rotation frequency,  $\omega(\rho)$  and  $\omega_{exp}(\rho)$ , at  $t = 11$  s for hybrid H-mode shot #60933 are shown in figure 1. We see their reasonable agreement. Figure 2 presents the temporal evolution of four deviations:  $d_2T_e$ ,  $d_2T_i$ ,  $d_2n$  and  $d_2\omega$  for the same shot. The first three deviations are calculated with the nonlinear model presented in section 5.2; the fourth deviation is obtained by the calculations with the linear model presented in section 5.1. The next figures illustrate the shot #52009 with the H-mode and rather high density. Figure 3 shows the temporal evolution of the total input NBI power  $P_{NBI}$ , line-averaged density  $\bar{n}$ , and experimental and calculated central electron temperatures,  $T_{ex0}$ ,  $T_{e0}$ . We see that the quasi-steady state phase in this shot lasts at least 6 s ( $17 \text{ s} < t < 23 \text{ s}$ ). Figure 4 shows the temporal evolution of the deviations of electron temperature, density and angular frequency in the same shot. During the rapid density ramp-up, the simulation procedure adjusts the calculated density with some delay, so the RMS density deviation  $d_2n$  is as large as 20%, and the deviations of temperature and frequency are also at the level of 20-25%. However, in the second part of steady state phase, for  $20 \text{ s} < t < 23 \text{ s}$ , the calculated density is reasonable ( $d_2n \sim 3\text{-}5\%$ ) and the temperature and frequency deviations decrease to the level of 5-10%. The next figure presents data for shot #52014 with very high density H-mode plasma. Such a high density leads to peripheral deposition of beam particles, which transfer their torque to plasma ions also at the periphery (figure 5). However, the experimental profile of angular frequency has maximum at the plasma center. Such plasma behaviour may be evidence of an anomalous momentum pinch, directed to the center. This momentum pinch is intrinsic in our model, when the first term in brackets for the momentum flux in (27) is less than the second one. Such an anomalous momentum pinch was seen in experiment also [14].

Figure 6 presents the momentum confinement time  $\tau_\omega$  (a) (Eq. (31)) and the ratio  $\tau_\omega/\tau_E$  (b) as functions of the plasma density for shots with rather high plasma currents ( $I_p > 1.5$  MA) at the quasi steady-state phase of discharges. At high densities the profiles of input power are hollow, and the energy rapidly escapes from plasma. However, owing to the strong pinch of angular momentum (illustrated by figure 5) the momentum confinement time increases during the density ramp-up. The ratio  $\tau_\omega/\tau_E$  grows from small values ( $\sim 0.5$ ) at low densities up to values exceeding unity ( $\sim 2$ ) at high densities.

Figure 7 shows RMS deviations of angular frequency  $d_2\omega$  averaged over the time intervals  $\Delta t \sim 1-2$  s for all 11 shots of Table 1, and ranked with plasma density. We see that the deviations are generally less than 10-15%. The next figure 8 characterizes the quality of simulation of the electron and ion temperatures and plasma density by nonlinear model (32)-(37). Here the RMS deviations  $d_2T_e$ ,  $d_2T_i$  and  $d_2n$  are shown for shots with enough high current  $I_p > 1.5$  MA. It is seen that the temperature deviations are of the level 10%, but the density deviations are approximately two times lower.

The developed model was applied to MAST experiment. For this device the coefficient  $C_\omega$  in (38), found from the analysis of 3 shots, is smaller:  $C_\omega = 0.5 / n^{1/3}$ . Figure 9 shows the profiles of deposited torque  $L$  (from TRANSP), calculated angular rotation frequency  $\omega$  and the experimental one,  $\omega_{\text{exp}}$ , for two MAST shots #13035 and #18696 with different densities. It is seen that for MAST the calculated and experimental profiles are also close one to another.

## CONCLUSIONS

The variational problem of minimizing plasma energy has allowed us to find the canonical profile of the toroidal rotation velocity. The transport model based on this canonical profile has been calibrated to describe reasonably the velocity of forced toroidal rotation of JET plasmas. The RMS deviations of calculated rotation profiles from the experimental ones do not exceed 10-15%. The application of the proposed model to the simulation of MAST rotation has shown the encouraging results.

## ACKNOWLEDGEMENTS

This work was partly carried out within the framework of the European Fusion Development Agreement Work, and partly funded by the UK EPSRC under grant EP/G003955 and the EC under the contract of Association between EURATOM and CCFE, and by Russian RFBR

Grant 08-07-00182. The views and opinions expressed herein do not necessarily reflect those of the European Commission.

## REFERENCES

- [1] de Vries P C *et al* 2006 *Nuclear Fusion* **46** 065006
- [2] Bateman G *et al* FEC-2008 22-nd IAEA Fusion Energy Conference “Integrated modeling simulations of toroidal momentum transport in tokamaks” paper TH/P8-35
- [3] Hsu J Y and Chu M S 1987 *Physics of Fluids* **30** 1221
- [4] Dnestrovskij Yu N *et al* 2010 *Plasma Physics Report* **36** 645
- [5] Kadomtsev B B 1987 *Soviet Journal of Plasma Physics* **13** 443
- [6] Dnestrovskij Yu N *et al* 2002 *Plasma Physics Report* **28** 887
- [7] Dnestrovskij Yu N, Dnestrovskij A Yu and Lysenko S E 2005 *Plasma Physics Report* **31** 529
- [8] Dnestrovskij Yu N *et al* 2007 *Plasma Physics and Controlled Fusion* **49** 1477
- [9] Dnestrovskij Yu N *et al* 1991 *Nuclear Fusion* **31** 1877
- [10] Dnestrovskij Yu N *et al* 1995 *Nuclear Fusion* **35** 1047
- [11] Politzer P A *et al* 2008 *Nuclear Fusion* **48** 075001
- [12] Mantica P *et al* 2009 *Physics Review Letters* **102** 175002
- [13] Roach C M *et al* 2008 *Nuclear Fusion* **48** 125001
- [14] Tala T *et al* 2009 *Physics Review Letters* **102** 075001

#		Current		Power		Density	Torque	Comment
		$I_p$ (MA)	$P$ (MW)	$n$ , ( $10^{19} \text{ m}^{-3}$ )	$T$ (N m)			
1	38285	2.5	12	6	11	H-mode		
2	38287	2.5	12	5	10	H-mode		
3	52009	2.5	15	7.5	14	H-mode		
4	52014	2.5	13.5	10.5	10	H-mode		
5	52015	2.5	13.5	10	12	H-mode		
6	52022	2.5	15	9	11.5	H-mode		
7	52024	2.5	15	10	11.5	H-mode		
8	52025	2.5	15	8.5	12.5	H-mode		
9	60927	1.4	13	3.5	13	Hybrid		
10	60931	1.4	17	3.5	17	Hybrid		
11	60933	2.0	15.5	3	22	Hybrid		

Table 1: Parameters of studied shots.

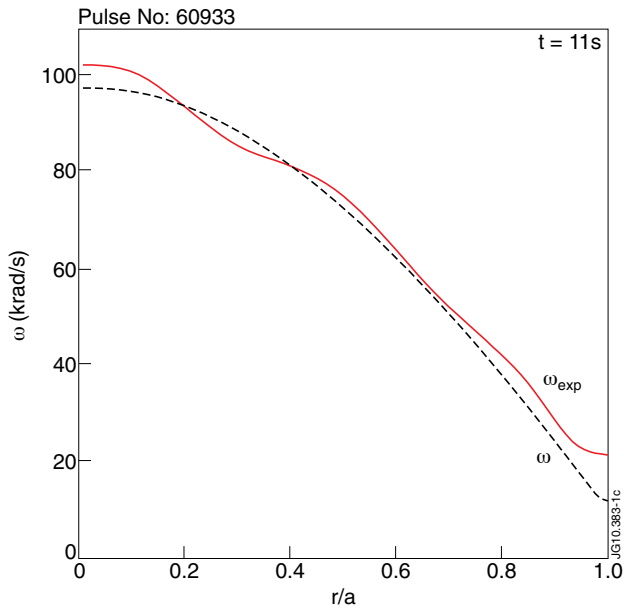


Figure 1: Calculated and experimental rotation frequencies for low-density JET shot.

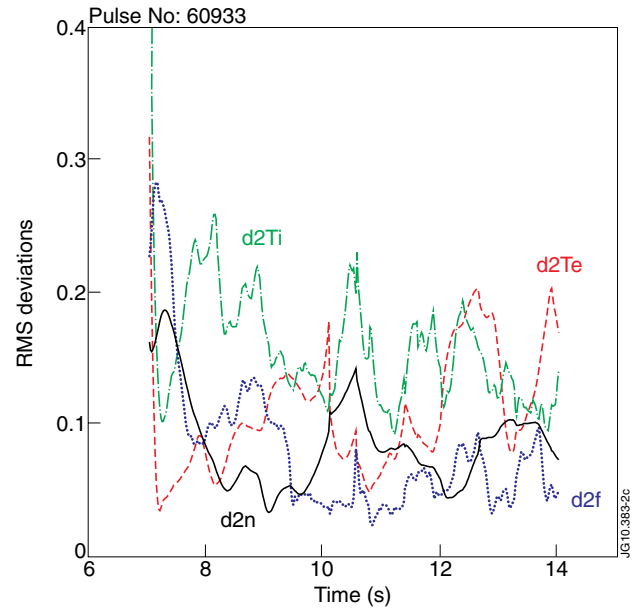


Figure 2: The temporal evolution of temperature, density and angular frequency deviations of calculations from experiment for the same shot.

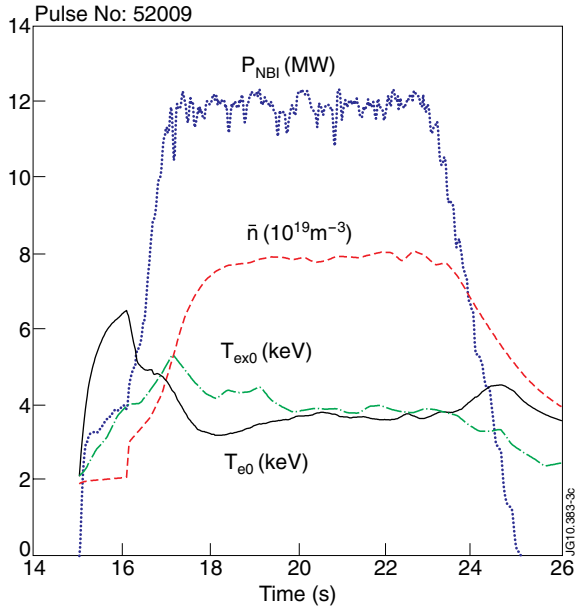


Figure 3: Temporal evolution of the NBI power  $P_{NBI}$ , line-averaged density  $\bar{n}$ , and experimental and calculated central electron temperatures,  $T_{ex0}$ ,  $T_{e0}$ , for the JET Pulse No:52009 with the H-mode and rather high density.

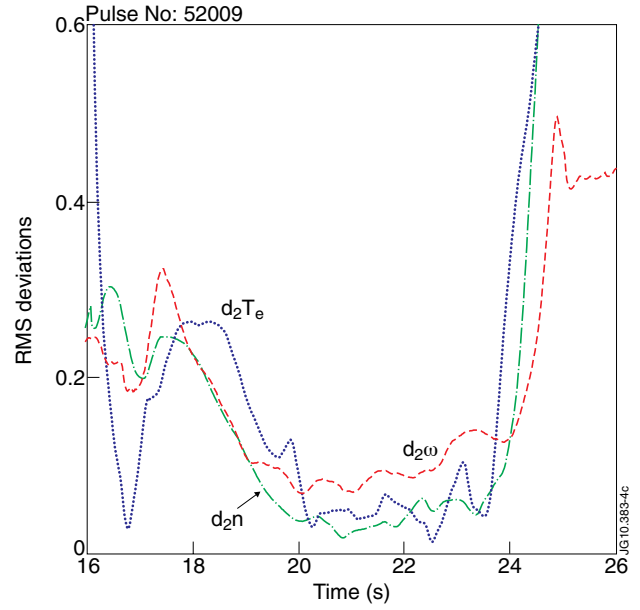


Figure 4: Deviations of the calculated electron temperature, density and angular frequency from experimental ones for the same JET shot.

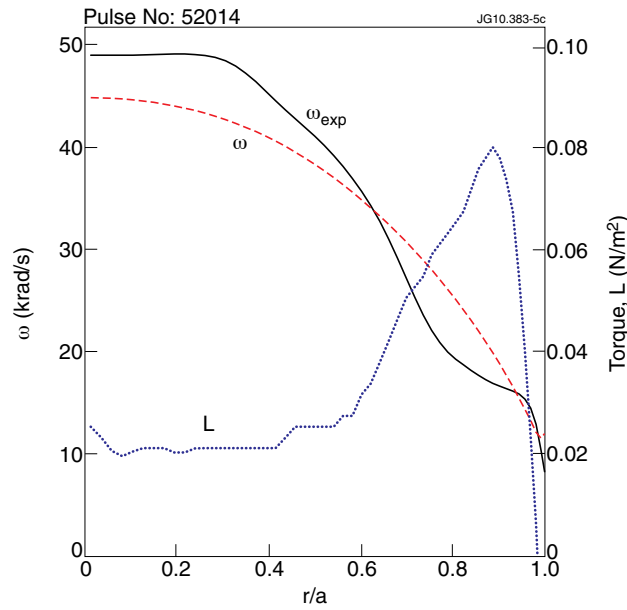


Figure 5: Profiles of experimental  $\omega_{exp}$  and calculated angular frequency  $\omega$ , and input specific torque L for high-density JET Pulse No: 52014 at  $t = 21s$ .



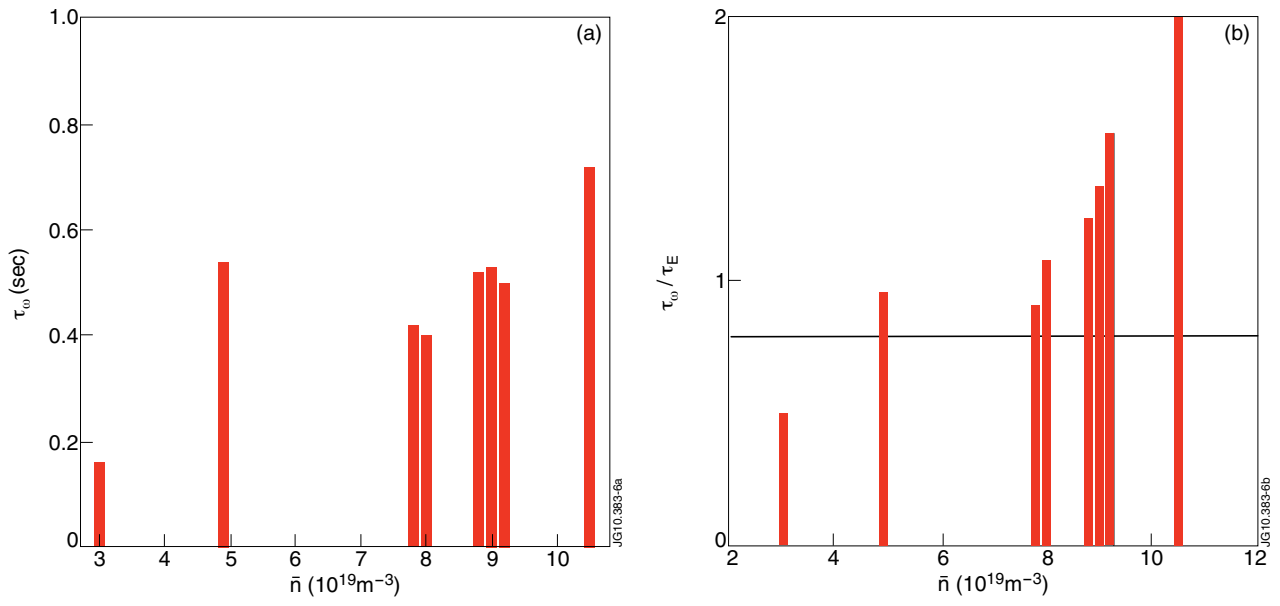


Figure 6: The momentum confinement time  $\tau_{\omega}$  (a) and the ratio  $\tau_{\omega}/\tau_E$  (b) as functions of the plasma density.

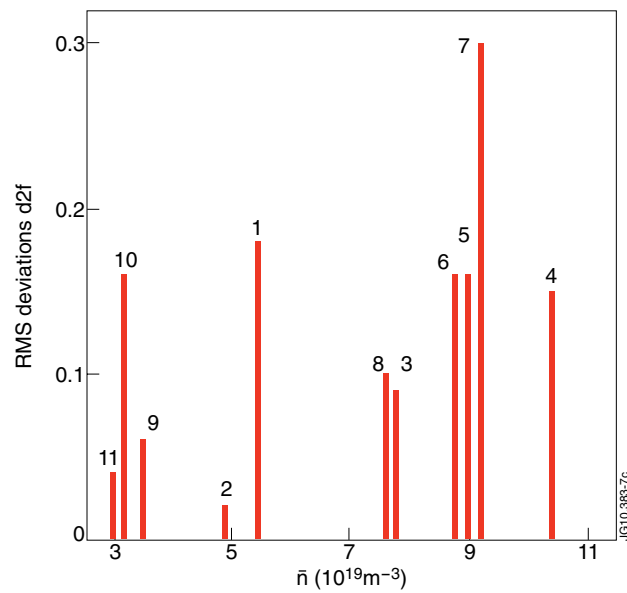


Figure 7: RMS deviations of angular frequency for 11 JET shots of Table 1.

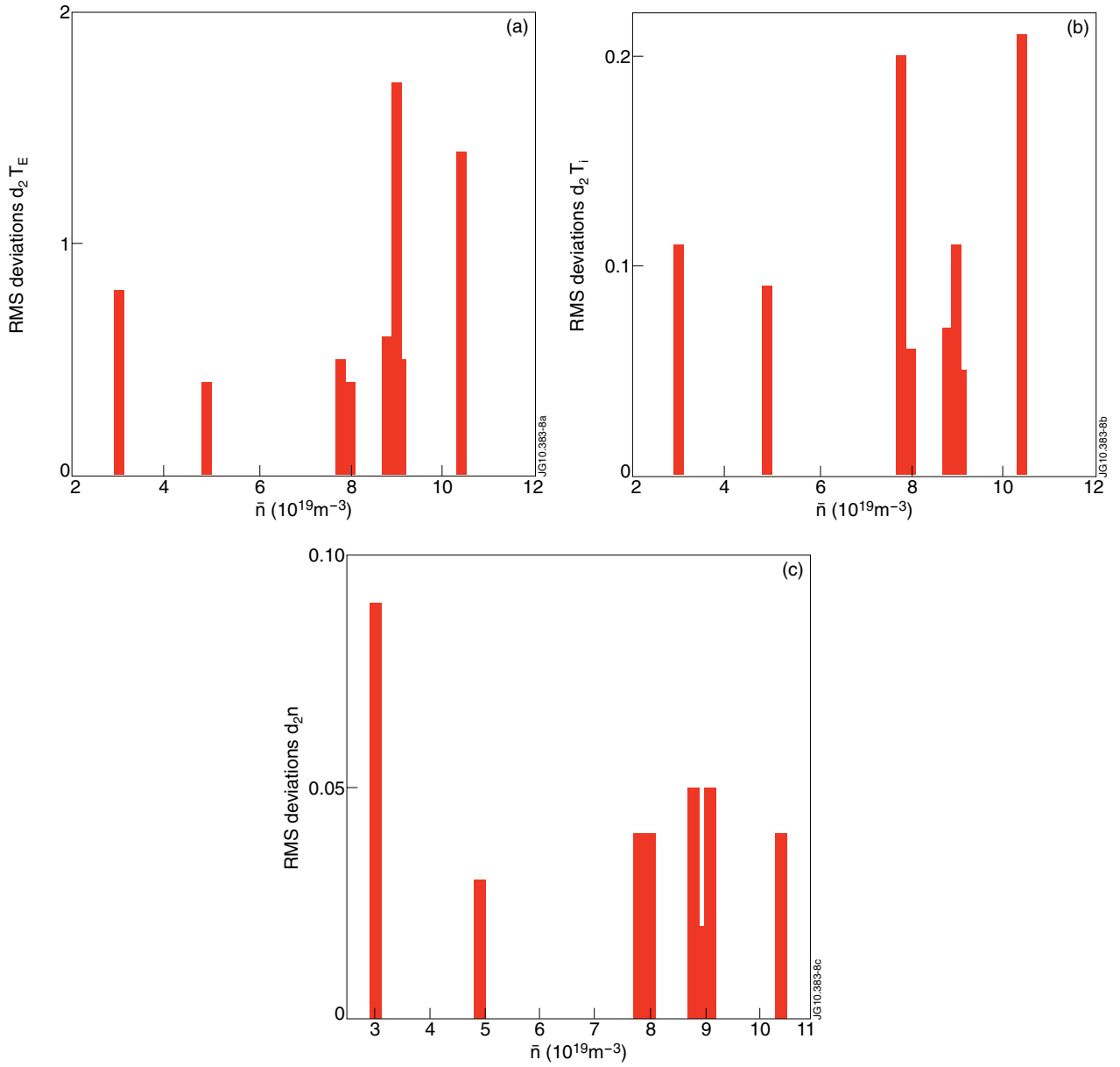


Figure 8: RMS deviations for JET shots with currents  $I_p > 1.5$  MA as functions of line-averaged density: (a) of electron temperature  $d_2 T_e$ , (b) of ion temperature  $d_2 T_i$ , and (c) of plasma density.

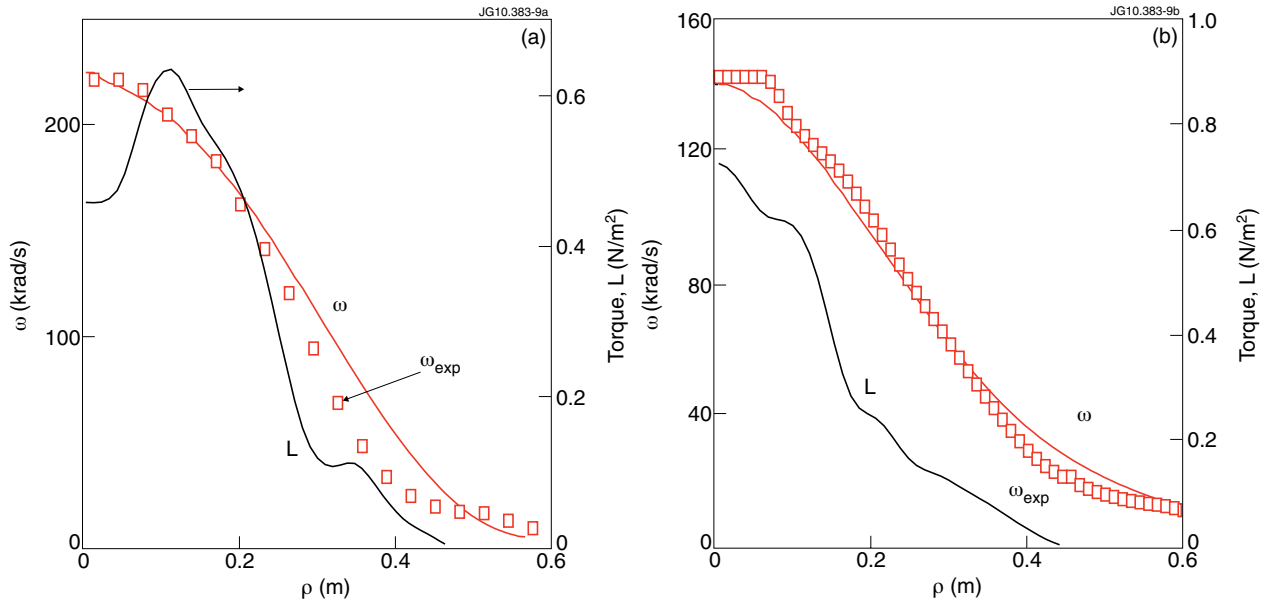


Figure 9: The profiles of deposited torque  $L$  from TRANSP, angular rotation frequency  $w$  from our model and experimental  $w_{exp}$  from TRANSP for two MAST shots with different line-averaged densities: Pulse No: 13035 with  $n = 2.7 \times 10^{19} \text{ m}^{-3}$  (a) and Pulse No: 18696 with  $n = 3.5 \times 10^{19} \text{ m}^{-3}$  (b).